

Effect of Gamma Radiation on the Surface and Bulk Properties of Poly(tetrafluoroethylene)

A. Yu. Obvintsev^{a, *}, N. V. Sadovskaya^a, S. A. Khatipov^b, and V. M. Buznik^c

^aKarpov Institute of Physical Chemistry, Moscow, 103064 Russia

^bNesmeyanov Institute of Organoelement Compounds, Russian Academy of Sciences, Moscow, 119991 Russia

^cAll-Russian Institute of Aviation Materials, Moscow, 105005 Russia

*e-mail: obvsun@mail.ru

Received February 2, 2017

Abstract—The effect of gamma radiation on the contact angle θ , the work of adhesion γ_{SL} for polar and non-polar liquids, disperse and polar components of the surface energy γ_S , the magnitude of bulk dielectric polarization P_0 , and the dielectric increment $\Delta\epsilon$ for sintered and non-sintered poly(tetrafluoroethylene) (PTFE) of suspension polymerization are studied. Sintered PTFE exhibits anomalously high growth of the studied parameters with an absorbed dose up to 500 kGy: $\Delta\epsilon$ by more than four orders of magnitude, the work of adhesion of the polar liquid $\gamma_{SL}^{\text{H}_2\text{O}}$ by a factor of 1.5, the polar component of the surface energy γ_S^{pol} by 20 times. The observed changes are found to be considerably larger than those expected from the viewpoint of the amplification of dipole–dipole and donor–acceptor molecular interactions with the participation of polar groups formed in poly(tetrafluoroethylene) upon irradiation. The similar behavior of $\Delta\epsilon$, $\gamma_{SL}^{\text{H}_2\text{O}}$, and γ_S^{pol} parameters depending on the exposed dose and subsequent annealing of the samples at 150°C is revealed. A unified mechanism for changes in the bulk polarization and surface properties caused by the formation in poly(tetrafluoroethylene) of long-lived electron–hole pairs is suggested.

Keywords: poly(tetrafluoroethylene), gamma irradiation, contact angle, surface energy, polar groups, dielectric increment

DOI: 10.1134/S1027451017050123

INTRODUCTION

The low surface energy of poly(tetrafluoroethylene) (PTFE) provides its high anti-adhesive properties but greatly limits its compatibility with other materials. Different methods of PTFE surface modification are used to design adhesive joints. The most efficient among them are defluorination by reducing agents, UV (ultraviolet) irradiation, and plasma treatment, which increases the surface energy of PTFE due to the acceptance of excess charge carriers and the formation of polar destruction products [1]. The development of methods to control the wettability of fluorine-containing polymers is important for practical applications [2].

Fillers for composites containing PTFE as a matrix are commonly modified to reduce their surface energy. This is achieved mainly by the grafting of perfluorocarbon fragments to the filler surface. A decrease in the filler surface energy leads to better incorporation into the fluoropolymer matrix and a reduction in the propensity to aggregation. This approach is exemplified by the chemical grafting of perfluoroalkylsilanes to silicon dioxide [3] and alumi-

num oxide [4] fillers, as well as the plasma-chemical deposition of perfluoroalkane coating on carbon fibers [5, 6].

In the case of a polymer–polymer composite, when PTFE behaves as a filler for a polar polymer matrix, surface defluorination of PTFE powder was used [7] to increase the surface energy and adhesion to the polar matrix. The exposure of PTFE powder to accelerated electrons was used for its subsequent application as a filler for polyamide [8, 9] and ethylene–propylene rubber [10].

It was shown by IR (infrared) spectroscopy [11–13], electron paramagnetic resonance [11, 12], and thermogravimetry [14, 15] that the exposure of PTFE powder to ionizing radiation leads to the formation of carbonyl, carboxyl, and carbonyl fluoride groups and long-lived peroxide macroradicals on the surface and in the bulk of particles. It was concluded in the works [11–13] that the emergence of polar groups in the structure of macromolecules is the main reason for the growth of the surface energy of irradiated PTFE. According to the conclusions of [13], the main contri-

Table 1. Contact angles of water for the studied samples before irradiation

Sample	F4PN	F4	F4RM
1	109.8	109.5	106.8
2	110.9	109.3	106.2
3	110.4	112.5	106.1
4	111.3	113.1	108.9
5	–	110.8	107.4
Average value	110.6	111.0	107.1

bution to growth in the surface energy of irradiated PTFE powder is provided by carboxyl groups.

Radiation-induced chemical processes in polymers, including the formation of radicals, neutral products, and charged particles, are dependent on structure. Therefore it is of interest to compare the effect of radiation on the surface energy of sintered and non-sintered PTFE. The crystal structure and morphology of PTFE powder is known [16] to change considerably upon sintering which is used in the preparation of goods. In this work, we study the effect of ^{60}Co gamma radiation on PTFE manufactured by suspension polymerization.

EXPERIMENTAL

Objects. To study non-sintered PTFE, F4PN samples, we used a powder of PN-grade (State standard 10007-80) suspension polymerization manufactured by the Galo-Polimer Corporation (Moscow) not subjected to heating to the crystallite melting temperature. The samples of F4PN for measurement of the contact angles and bulk currents of electric depolarization were fabricated as disks 50 mm in diameter and 1 mm thick by the uniaxial compaction of PTFE powder after accumulation of the given absorbed radiation dose.

The samples of sintered PTFE, samples F4, for measurement of the contact angles were fabricated from a powder of suspension polymerization of PN grade (State standard 10007-80) manufactured by the Galo-Polimer Corporation (Moscow) as $25 \times 15 \times 15$ mm bars via uniaxial compaction under a pressure of 30 MPa followed by annealing at 380°C (specification TU 6–05–810).

A portion of the bars of the sintered PTFE obtained by the above technique were subjected to preliminary radiation modification using ^{60}Co gamma rays at a temperature above the melting point at an absorbed dose of 200 kGy (samples F4RM). According to [16], the supramolecular structure of F4RM differs considerably from the structure of F4.

The bulk current of the electric polarization of F4 and F4RM was measured for samples as disks of 50 mm in diameter and 1 mm thick fabricated from a

powder of PN-grade (State standard 10007-80) suspension polymerization of manufactured by the Galo-Polimer Corporation (Moscow) via uniaxial compaction under 30-MPa pressure followed by annealing at 380°C (specification TU 6-05-810).

Surface preparation. Great attention was paid to the preparation of samples to measure the contact angles because their values are considerably affected by the purity, imperfection, and roughness of the studied surface. To remove processing impurities and defects from one of the surfaces of the F4 and F4RM samples manufactured as bars $25 \times 15 \times 15$ mm in size, a layer about 1 mm thick was cut by a microtome. Next, to reduce the roughness, this surface was pressed to an optical glass plate (State standard 2786-82) and kept at a constant pressure at 150°C for 4 h. To provide minimal roughness of the surface of the samples F4PN obtained as disks 1 mm thick by pressing the initial and irradiated powders, we used optical glass as one of the punches.

The surface quality was monitored by the values of the contact angles of water. It is known [17] that these values for PTFE should be about 110° in the case of careful preparation of surface. Table 1 shows that the studied surfaces of F4 and F4PN samples are close to this value. A decrease in the average value of the contact angles for F4PN by 4° as compared with F4 is expected and caused by its preliminary radiation-induced modification in melt resulting in slight growth of the surface energy.

Irradiation. The samples were obtained using an RV-1200 gamma-ray installation in air at ambient temperature at an absorbed dose rate of 0.65 Gy/s.

Measurement of the contact angles. The contact angles were measured by the sessile drop technique on a KRUSS EasyDrop instrument using DSA1v1.92 software. The droplet volume was 4 μL . The contact angles were calculated by the software accompanying the instrument. The contact angles for each sample were measured at five different points of the surface. The obtained data were averaged over all points.

The contact angle for the sessile drop is determined by Young's law:

$$\cos \theta = \frac{\sigma_S - \sigma_{SL}}{\sigma_L}, \quad (1)$$

where θ is the contact angle, σ_S , σ_L , σ_{SL} are the surface tension at the solid–gas, liquid–gas, and solid–liquid phase boundary, respectively.

The work of adhesion γ_{SL} was determined by the formula (2):

$$\gamma_{SL} = \sigma_L(1 + \cos \theta). \quad (2)$$

The surface tension σ_L was taken to be 72.8 mJ/m^2 for water and 26.7 mJ/m^2 for tetradecane [18].

The disperse and polar parts of the surface energy were determined by the Owens–Wendt method using

polar and non-polar liquids. For this purpose, we used deionized water and chromatographically pure tetradecane. The component values were calculated by the standard program applied to the KRUSS EasyDrop instrument.

Density measurement. The density of the studied samples was determined by hydrostatic weighing at an air and water temperature of 22°C. Sample weight in air and in distilled water was measured using Vibra HJR-620CE scales (Japan) in steps of 1.0 mg. The density was calculated by the formula:

$$\rho = \frac{\rho_w m_0}{m_0 - m_w}, \quad (3)$$

where ρ is the sample density in g/cm^3 , ρ_w is the density of distilled water at the given temperature, m_0 and m_w are the sample weights in air and water, respectively. The density was determined by averaging the independent measurements (at least three) for each sample. The measurement error for the density was $\pm 0.001 \text{ g/cm}^3$.

Depolarization current measurement. To study polarization effects, we used the method of isothermal drop in the polarization and depolarization current. The method is based on the recording of transient electric current under isothermal conditions after stepwise switching on/off of the external electric field. The charging current upon switching-on the external electric field is the sum of the polarization and conduction currents, the discharging current upon switching-off the electric field is determined only by the depolarization current and directed oppositely to the charging current. The measurement scheme is presented in Fig. 1.

Upper and lower electrodes 36 and 28 mm in diameter were applied on disks 2 mm thick using electrically conducting paint. The electric-field strength was given as 10^6 V/m . The charging time was 300–400 s.

The dielectric increment $\Delta\epsilon$ was calculated from measurement of the depolarization currents [19]:

$$\Delta\epsilon = \frac{P_0}{\epsilon_0 E}, \quad (4)$$

where $P_0 = \int_0^\infty J(t)dt$ is the value of the total polarization, $J(t)$ is the depolarization current density, E is the electric-field strength, $\epsilon_0 = 8.85 \times 10^{-12} \text{ F/m}$ is the dielectric constant.

RESULTS AND DISCUSSION

Figures 2 and 3 display the dependences of the contact angle θ for water and tetradecane on the absorbed dose for samples F4PN, F4, and F4RM. The relatively small change in the contact angle of water on F4PN powder is noteworthy: the contact angle decreases by 7.5° at a maximal absorbed dose of 500 kGy. These changes for sintered samples F4 and F4RM are con-

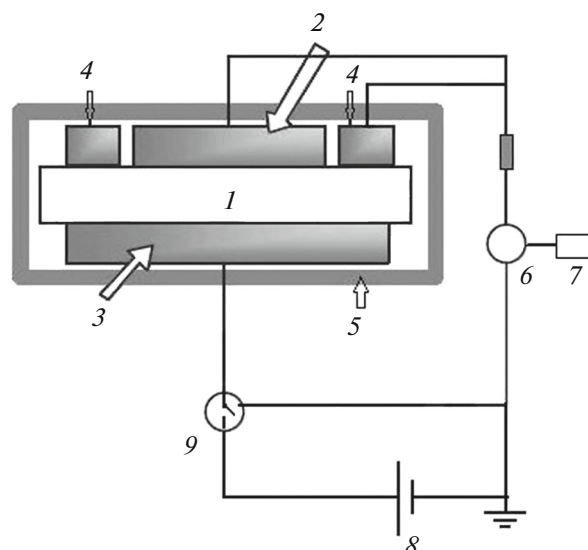


Fig. 1. Scheme of measurement of isothermal polarization/depolarization currents: 1, sample; 2, measuring electrode; 3, high-voltage electrode; 4, guard electrode; 5, measuring chamber; 6, V7E-42 electrometric amplifier; 7, recorder; 8, BNV2-95 power supply unit; 9, measurement mode switcher.

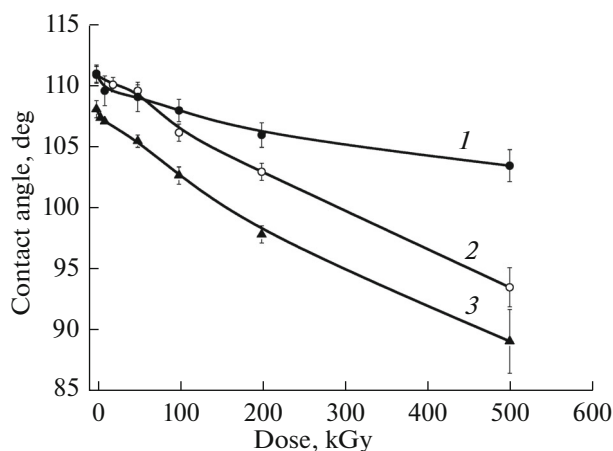


Fig. 2. Contact angle of water depending on the exposure dose for samples: 1, F4PN; 2, F4; 3, F4RM.

siderably larger and close to each other: 17.3° and 18.9° , respectively. All of the contact angles of water for the F4PN powder which depend on the absorbed dose are considerably higher than those for a similar powder of TF 1750 grade [13]. The decrease of θ for the TF 1750 powder at dose 500 kGy was about 25° . In [13], preliminary pressed samples of powder were exposed to radiation, their density and porosity were closer to sintered PTFE than to the initial powder.

Such a considerable difference in the contact angle of polar liquid for the non-sintered powder of F4PN, sintered F4 and F4RM samples, and the preliminarily

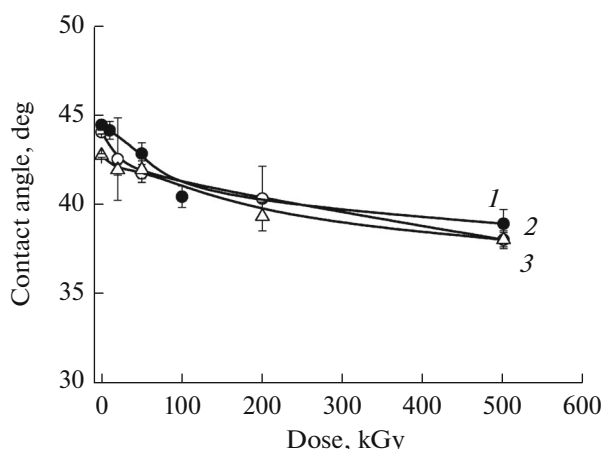


Fig. 3. Contact angle of tetradecane depending on the exposure dose for samples: 1, F4PN; 2, F4; 3, F4RM.

pressed powder of TF 1750 could not be explained by a difference in the polar-group concentration.

Indeed, the decrease in the degree of crystallinity, as a rule, increases the radiation-chemical yield of

Table 2. Dispersive and polar components of the PTFE surface energy (γ_S^{dis} and γ_S^{pol}) calculated by the Owens–Wendt method using experimental values of the work of adhesion for water and tetradecane ($\gamma_{SL}^{\text{H}_2\text{O}}$ and $\gamma_{SL}^{\text{C}_{14}\text{H}_{30}}$) depending on the absorbed radiation dose

Sample	γ_S^{dis}	γ_S^{pol}	$\gamma_S^1)$	$\gamma_{SL}^{\text{H}_2\text{O}}$	$\gamma_{SL}^{\text{C}_{14}\text{H}_{30}}$
F4PN-0	19.62	0.15	19.77	47.0	45.8
F4PN-10	19.70	0.24	19.95	48.5	45.9
F4PN-50	20.06	0.26	20.32	49.1	46.3
F4PN-100	20.71	0.31	21.02	50.4	47.1
F4PN-200	20.71	0.53	21.24	52.9	—
F4PN-500	21.11	0.83	21.94	55.9	47.5
F4-0	19.73	0.15	19.88	47.0	45.9
F4-20	20.15	0.18	20.32	47.9	46.3
F4-50	20.36	0.20	20.56	52	47.6
F4-100	20.36	0.54	20.90	52.6	—
F4-200	20.74	0.96	21.70	56.5	47.7
F4-500	21.34	3.12	24.46	68.4	47.7
F4RM-0	20.09	0.35	20.44	50.3	46.3
F4RM-5	20.09	0.42	20.51	51.2	—
F4RM-10	20.09	0.46	20.55	51.5	—
F4RM-20	20.31	0.56	20.87	—	46.6
F4RM-50	20.31	0.64	20.94	53.5	46.6
F4RM-100	20.58	1.04	21.62	56.9	—
F4RM-200	21.00	1.99	22.99	62.9	47.4
F4RM-500	21.34	4.56	25.99	73.9	47.7

¹⁾ $\gamma_S = \gamma_S^{\text{dis}} + \gamma_S^{\text{pol}}$ is the total surface energy. All values have a dimension of mJ/m^2 .

polymer-chain destruction products. Therefore, for sintered samples of F4 and F4RM, whose crystallinity is lower than that of the powders, the effect of irradiation on the contact angle should be larger than for TF 1750 due to a higher concentration of polar groups. However, there is no such correlation. On the other hand, the crystallinity of TF 1750 and F4PN powders is almost the same, but samples with different porosity and hence gas permeability were exposed to radiation. The concentration of oxygen-containing groups should be higher in the case of F4PN samples that were not pressed due to a higher gas permeability, while the decrease in the contact angle should be larger than for TF 1750. This effect is not observed too. The effect of molecular structure on radiation-chemical processes is not considered in this case because the studied samples do not differ in terms of this feature.

In the case of a dispersive liquid, the change in the contact angles upon irradiation is independent of the sample microstructure (Fig. 3). The differences in the contact angles for the initial and irradiated samples at 500 kGy are close to each other and equal to 5.5° , 6° , and 4.7° for F4PN, F4, and F4RM, respectively.

Table 2 displays the work of adhesion for water $\gamma_{SL}^{\text{H}_2\text{O}}$ and tetradecane $\gamma_{SL}^{\text{C}_{14}\text{H}_{30}}$ calculated with the use of relationship (2) depending on the radiation dose and the values of the dispersive and polar components of the surface energy γ_S^{dis} and γ_S^{pol} calculated by the Owens–Wendt method. The presented data indicate two important features. The first feature: relative changes in the work of adhesion for the dispersive liquid are always small; they are within 5% at a maximal dose of 500 kGy, whereas they reach 50% for the polar liquid for F4RM and 20% for F4PN powder. The work of adhesion of water on the F4RM surface at 500 kGy equal to $73.9 \text{ mJ}/\text{m}^2$ (Table 2) is close to the corresponding value for a polar polymer, i.e., polystyrene (PS), which is $84 \text{ mJ}/\text{m}^2$ [20].

The second feature is caused by an anomalously large increase in the polar component of the surface energy for F4 (by 20 times at 500 kGy) and F4RM (by more than 10 times at 500 kGy) (Table 2). The polar component γ_S^{pol} for F4 and F4RM reaches 3.12 and $4.65 \text{ mJ}/\text{m}^2$ (Table 2), which is higher than the corresponding value for polar PS of $3 \text{ mJ}/\text{m}^2$ [20]. The dispersive component in this case slightly increases up to 10%.

Very high values of γ_S^{pol} for the irradiated samples of F4 and F4RM could not be explained only by the formation and accumulation of polar groups because their concentration even at the maximal possible radiation-chemical yield ($10\text{--}1/100 \text{ eV}$) is several orders of magnitude lower than the dipole concentration in a polar polymer, including PS, while their dipole moment could not be larger by the same orders of magnitude.

Table 3. Contact angles θ of water (H_2O) and tetradecane ($\text{C}_{14}\text{H}_{30}$) for samples F4 and F4RM depending on the absorbed dose before and after annealing at 150°C

Sample	$\theta(\text{H}_2\text{O})$, deg		$\theta(\text{C}_{14}\text{H}_{30})$, deg	
	before annealing	after annealing	before annealing	after annealing
F4-0	110.0	109.9	44.0	42.8
F4-200	102.9	110.0	40.3	32.0
F4-500	93.5	108.8	38.0	32.1
F4RM-0	108	106.8	42.7	42.4
F4RM-200	97.8	107.4	39.3	35.6
F4RM-500	89.1	108.7	38.0	32.0

Table 4. Dispersive and polar components of the surface energy of PTFE (γ_S^{dis} and γ_S^{pol}) calculated by the Owens–Wendt method depending on the absorbed radiation dose before and after annealing at 150°C

Sample	Before annealing				After annealing			
	γ_S^1	γ_S^{dis}	γ_S^{pol}	ρ	γ_S^1	γ_S^{dis}	γ_S^{pol}	ρ
F4-0	19.88	19.73	0.15	2.148	20.25	20.24	0.01	2.149
F4-200	21.70	20.74	0.96	2.213	22.85	22.80	0.05	2.231
F4-500	24.46	21.34	3.12	2.225	22.84	22.77	0.07	2.240
F4RM-0	20.17	19.79	0.38	2.190	20.64	20.17	0.47	2.198
F4RM-200	22.99	21.00	1.99	2.200	22.20	21.94	0.26	2.205
F4RM-500	25.99	21.34	4.65	2.203	22.91	22.80	0.11	2.213

¹⁾ $\gamma_S = \gamma_S^{\text{dis}} + \gamma_S^{\text{pol}}$ is the total surface energy. All values have the dimension of mJ/m^2 .

It should be noted that the polar component of the surface energy of a solid determined by the Owens–Wendt method was interpreted in [21] as a result of hydrogen bonding upon contact with a polar liquid. In the more modern Van Oss–Good model [22], this non-dispersive contribution is called “donor–acceptor” or “acid–base” (in terms of Lewis acidity and basicity). Therefore, one can suppose that the high values of γ_S^{pol} for irradiated F4 and F4RM are caused by not only the dipole–dipole interactions of polar groups but also hydrogen bonds that arise upon the contact of water with carbonyl and carboxyl groups.

It is known [23] that the concentration of these groups changes upon the annealing of irradiated samples within $100\text{--}200^\circ\text{C}$. Annealing at 200°C in air leads to increase in the number of free and bound COOH groups by $50\text{--}100\%$. Therefore in this work, we studied the effect of annealing in air on the contact angles of water and tetradecane for the initial and irradiated samples of F4 and F4RM, which showed the largest radiation-induced effects.

Table 3 shows that the annealing of samples at 150°C leads to complete restoration of the initial values of the contact angles of water, whereas the angles of tetradecane show a trend to a further decrease. The polar component of the surface energy γ_S^{pol} calculated by the Owens–Wendt method sharply decreases, while the dispersive component γ_S^{dis} slightly increases

(by less than 10%, Table 4). The work of water adhesion $\gamma_{SL}^{\text{H}_2\text{O}}$ to the surface of irradiated F4 and F4RM samples returns to the initial values after annealing, while the work of tetradecane adhesion $\gamma_{SL}^{\text{C}_{14}\text{H}_{30}}$, like that of γ_S^{dis} , slightly increases (Figs. 4 and 5).

The character of changes in $\gamma_{SL}^{\text{C}_{14}\text{H}_{30}}$ and γ_S^{dis} after the annealing of irradiated samples is regular and can be explained by an increase in the sample density (Table 4) and the number of polar groups. Indeed, it is known [24] that the annealing of PTFE irradiated in air at $100\text{--}200^\circ\text{C}$ is accompanied by post-oxidative destruction under favorable conditions (at an excess concentration of molecular oxygen) in the chain reaction mode. The reaction sequence is associated with the monomolecular decomposition of peroxide macroradicals to give low-molecular-weight oxygen-containing perfluorocarbons, terminal carbonyl fluoride groups, and double bonds. Each act of decomposition of a terminal peroxide radical restores a terminal fluoroalkyl radical, which combines with an oxygen molecule to give a peroxide radical again. In the presence of water vapors on the surface of the powder particles and sintered samples, additional COOH groups form due to the hydration of carbonyl-fluoride groups. An increase in the density upon annealing proceeds due to a further decrease in the molecular weight and increase in the sample crystallinity. An increase in the

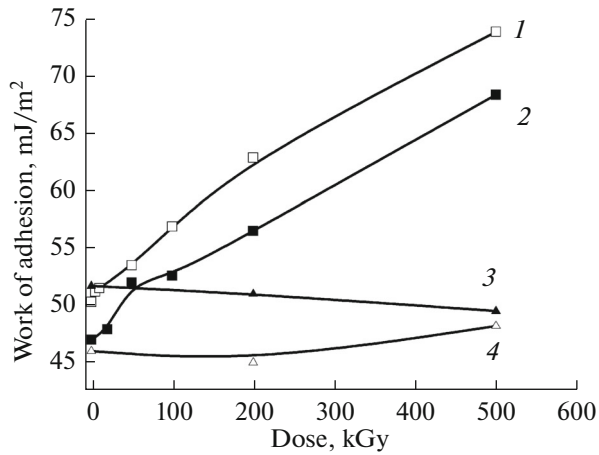


Fig. 4. Work of water adhesion to the surface of the samples F4RM (1, 3) and F4 (2, 4) depending on the exposure dose before (1, 2) and after annealing at 150°C (3, 4).

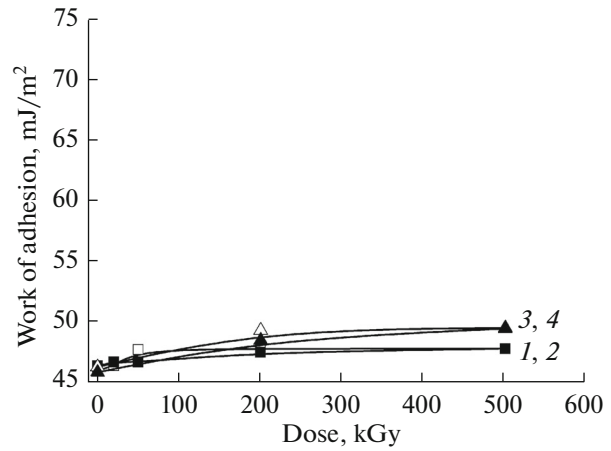


Fig. 5. Work of tetradecane adhesion to the surface of the samples F4RM (1, 3) and F4 (2, 4) depending on the exposure dose before (1, 2) and after annealing at 150°C (3, 4).

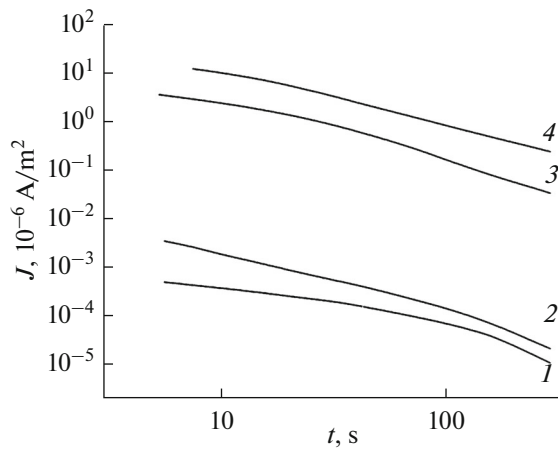


Fig. 6. Time dependence of the isothermal depolarization current for the initial F4 sample (1) and samples F4PN (2), F4 (3), and F4RM (4) exposed to dose 50 kGy.

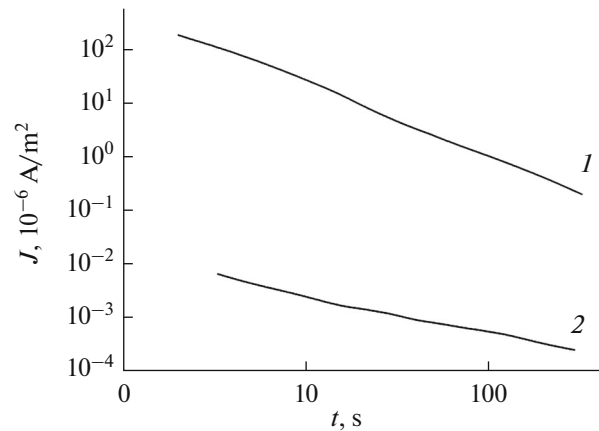


Fig. 7. Time dependence of the isothermal depolarization current for the F4 sample exposed to 100 kGy dose before (1) and after annealing at 150°C (2).

density and number of polar groups upon both irradiation and subsequent annealing favors the amplification of dispersive interactions, which agrees qualitatively with the character of changes in $\gamma_{SL}^{C_{14}H_{30}}$ and γ_S^{dis} .

Moreover, the behavior of the work of adhesion $\gamma_{SL}^{H_2O}$ and polar component γ_S^{pol} upon annealing is opposite to that expected. Instead of an increase in these parameters due to a growth in the number of COOH groups and other polar groups, one observes their decrease to a level typical for initial non-irradiated samples. This feature provides no possibility to interpret the changes of $\gamma_{SL}^{H_2O}$ and γ_S^{pol} as a consequence of the amplification of dipole–dipole and donor–acceptor interactions on account of polar groups formed in irradiated PTFE.

Polar groups result from the secondary reactions of radicals that form during the first stages of radiation

impact on a polymer. The ionization of macromolecules at primary stages precedes radical formation. In contrast to the majority of polymers, PTFE is characterized by the stabilization of long-lived charged particles (electrons and holes) within the polymer matrix, the particles can be subjected to polarization in an electric field to give unusually high growth of the dielectric permittivity, dielectric loss factor, and dielectric increment $\Delta\epsilon$ [25–27]. Moreover, the annealing of samples in the range 100–200°C leads to the recombination of electron–hole pairs and restoration of the dielectric characteristics to the initial values [25]. It is noteworthy that the dielectric characteristics, work of adhesion $\gamma_{SL}^{H_2O}$, and polar component γ_S^{pol} of irradiated PTFE exhibit a similar behavior.

To reveal the possible role of stabilized charge carriers in the change in the surface energy, we measured the electric polarization/depolarization currents for

Table 5. Dielectric increment $\Delta\epsilon$ and total polarization P_0 before and after annealing of the samples at 150°C at different radiation doses

Sample	Before annealing		After annealing	
	$\Delta\epsilon$	$P_0, \text{C/m}^2$	$\Delta\epsilon$	$P_0, \text{C/m}^2$
PN-0	$<10^{-3}$	$<10^{-8}$		
PN-50	0.63×10^{-2}	5.6×10^{-8}	—	—
PN-100	0.58×10^{-2}	5.1×10^{-8}		
F4-0	$<10^{-3}$	$<10^{-8}$		
F4-50	22	1.9×10^{-4}	$<10^{-3}$	$<10^{-8}$
F4-100	40	3.5×10^{-4}	$<10^{-3}$	$<10^{-8}$
F4RM-0	<0.001	$<10^{-8}$		
F4RM-50	36	3.2×10^{-4}	$<10^{-3}$	$<10^{-8}$
F4RM-100	60	5.3×10^{-4}	$<10^{-3}$	$<10^{-8}$

the F4PN, F4, and F4RM samples after irradiation and annealing.

The obtained data confirm the similarity of the behavior of $\Delta\epsilon$, $\gamma_{SL}^{\text{H}_2\text{O}}$, and γ_S^{pol} depending on the radiation dose. The value of $\Delta\epsilon$ and the depolarization currents $J(t)$, like the $\gamma_{SL}^{\text{H}_2\text{O}}$ and γ_S^{pol} values, for non-sintered F4PN powder are considerably lower than that for the sintered samples of F4 and F4RM (Fig. 6, curves 2–4, Table 5). At an absorbed dose of 100 kGy, the depolarization currents and $\Delta\epsilon$ for F4 and F4RM increase as compared with the unirradiated samples by four–five orders of magnitude (Fig. 6, curves 1, 3, 4, Table 5). The annealing of samples at 150°C leads to a decrease in $\Delta\epsilon$ and the depolarization currents to the initial values (Fig. 7, Table 5). Similar behavior was observed for $\gamma_{SL}^{\text{H}_2\text{O}}$ and γ_S^{pol} .

CONCLUSIONS

The obtained results indicate the single nature of changes in the dielectric characteristics, the work of adhesion $\gamma_{SL}^{\text{H}_2\text{O}}$, and the polar component of the surface energy γ_S^{pol} upon the irradiation of PTFE due to the formation of long-lived charge carriers (electrons and holes) within the bulk polymer.

Polar radiolysis products affect mainly the work of the adhesion of the dispersive liquid $\gamma_{SL}^{\text{C}_{14}\text{H}_{30}}$ and the dispersive portion of the surface energy γ_S^{dis} , while charged particles determine the change in the work of adhesion for the polar liquid and change in the polar component of surface energy.

REFERENCES

1. R. H. Dahm and D. M. Brewis, *Rapra Review Report 183: Adhesion to Fluoropolymers* (Smithers Rapra Press, 2005).
2. V. M. Buznik, *Aviats. Mater. Tekhnol.*, No. 1, 29 (2013).
3. J. T. Fields and A. Garton, *Polym. Compos.* **17** (2), 242 (1996).
4. D. L. Burris, S. Zhao, R. Duncan, et al., *Wear* **267**, 653 (2009).
5. V. A. Shelestova, O. R. Yurkevich, and P. N. Grakovich, *Polym. Sci., Ser. B* **44** (3–4), 94 (2002).
6. V. A. Shelestova, P. N. Grakovich, S. G. Danchenko, and V. A. Smirnov, *Khim. Neftegazov. Mashinostr.*, No. 11, 39 (2006).
7. A. Shojaei and S. Gholamalipour, *Macromol. Res.* **19** (6), 613 (2011).
8. D. Lehmann, B. Hupfer, U. Lappan, et al., *Des. Monomers Polym.* **5** (2), 317 (2002).
9. G. Pompe, L. Häußler, G. Adam, et al., *Appl. Polym. Sci.* **98**, 1317 (2005).
10. M. Khan, R. Sohail, U. Franke, et al., *Wear* **266**, 175 (2009).
11. M. Khan, D. Lehmann, and G. Heinrich, *eXPRESS Polym. Lett.* **2** (4), 284 (2008).
12. K. Lunkwitz, W. Bürger, U. Geißler, et al., *Appl. Polym. Sci.* **60**, 2017 (1996).
13. W. Burger, K. Lunkwitz, G. Pompe, et al., *Appl. Polym. Sci.* **48**, 1973 (1993).
14. U. Lappan, G. Pompe, and K. Lunkwitz, *Appl. Polym. Sci.* **66**, 2287 (1997).
15. K. Schierholz, U. Lappan, and K. Lunkwitz, *Nucl. Instrum. Methods Phys. Res., Sect. B* **151**, 232 (1999).
16. S. A. Khatipov, S. A. Serov, N. V. Sadovskaya, and E. M. Konova, *Polym. Sci., Ser. A* **54** (9), 684 (2012).
17. H. W. Fox and W. A. Zisman, *J. Colloid Sci.* **5** (6), 514 (1950).
18. B. D. Summ and Yu. V. Goryunov, *Physical and Chemical Foundations of Wetting and Spreading* (Khimiya, Moscow, 1976) [in Russian].
19. B. I. Sazhin, *Electrical Properties of Polymers* (Khimiya, Leningrad, 1986) [in Russian].
20. Yu. G. Bogdanova, *Adhesion and its Role for Securing Polymer Composites' Strength* (Moscow State Univ., Moscow, 2010) [in Russian].
21. D. K. Owens and R. C. Wendt, *Appl. Polym. Sci.* **13**, 1741 (1969).
22. C. J. Van Oss, M. K. Chaudhury, and R. Good, *Chem. Rev.* **88**, 927 (1988).
23. U. Lappan, B. Fuchs, U. Geißler, et al., *Polymer* **43**, 4325 (2002).
24. V. K. Milinchuk, E. R. Klinshpont, and S. Ya. Pshchetskii, *Macroradicals* (Khimiya, Moscow, 1980) [in Russian].
25. S. A. Khatipov, *High Energy Chem.* **35** (5), 291 (2001).
26. S. A. Khatipov, Yu. R. Zhutayeva, N. A. Smirnova, and V. P. Sichkar, *Nucl. Instrum. Methods Phys. Res., Sect. B* **151**, 324 (1999).
27. S. A. Khatipov, Yu. R. Zhutaeva, and V. P. Sichkar', *Polym. Sci., Ser. B* **40** (11–12), 407 (1998).

Translated by I. Kudryavtsev